

Received August 27, 2020, accepted October 23, 2020, date of publication November 2, 2020, date of current version November 11, 2020.

Digital Object Identifier 10.1109/ACCESS.2020.3035166

A Comparative Study of Five Networks for Reservoir Classification Based on Geophysical Logging Signals

KAI ZHU¹, YONGHUI DU², QIAN WANG², NAIHUA JI¹, AND LI ZHANG¹

¹School of Information and Control Engineering, Qingdao University of Technology, Qingdao 266000, China

²Research Institute of Shaanxi Yanchang Petroleum (Group) Company Ltd., Xi'an 710075, China

Corresponding author: Kai Zhu (zhu_kaicom@163.com)


This work was supported in part by the Shandong Provincial Natural Science Foundation of China under Grant ZR2019PEE013, and in part by the Shandong Provincial Old and New Kinetic Energy Conversion Major and Key Project "Research and Development of Artificial Intelligence Interactive Cloud Service Platform for Intelligent Life" under Grant 201905200432.

ABSTRACT Unconventional reservoir classification suffers low accuracy because of the complex geophysical properties. With good performance and moderate cost, geophysical logging is considered to be of great potential as the compromise solution between seismic and core. Since the "sweet-spot" depending on the sands' properties are implied not in the logging "point" but "segment", 1D-CNN is supposed to be a better fit for reservoir classification: It doesn't pay too much attention to the logging signal sequence itself like LSTM, but focuses on feature extraction from the whole signals combination. Moreover, samples would have various sizes because of different layer thickness. While 1D-CNN requires all samples must be converted to a uniform size before input. 1D fully convolutional network (1D-FCN) can receive any size input of layer thickness without manually aligning it to the same size. For the first time in this paper, structures of the five networks including two fully connected networks (global mapping artificial neural network, GM-ANN and point-to-point mapping artificial neural network, PPM-ANN), two fully convolutional networks (1D fully convolutional network with decision-level fusion, 1D-FCN-DEF and 1D fully convolutional network with data-level fusion, 1D-FCN-DAF) and the common 1D convolutional neural network (1D-CNN) are compared and evaluated the suitability for processing logging data in detail. Results on tight gas in Ordos basin of China illustrated by receiver operating characteristics (ROC) curves show that 1D-FCN-DEF and 1D-FCN-DAF have achieved the higher area under the curve (AUC) with the values of 0.8889 and 0.9107 respectively in average comparing to 0.7515, 0.8006 and 0.8364 of GM-ANN, PPM-ANN and 1D-CNN. Case study proves that 1D-FCNs are more accurate than other networks. This paper provides a suitable new idea for logging interpretation and expands the application scope of DL in geophysical logging signals processing.

INDEX TERMS Unconventional reservoir classification (URC), geophysical logging signals, 1D fully convolutional network (1D-FCN), 1D convolutional neural network (1D-CNN).

I. INTRODUCTION

Reservoir classification (RC) and hydrocarbon detection are the ultimate goal of geophysical exploration. Reservoir classification often suffers low accuracy for unconventional reservoirs (such as shale, coal-bed, tight sand etc.) due to their complex lithology, ultra-low permeability and complex fluid distribution. Seismic data has too large scales to describe hydrocarbon distribution of unconventional reservoirs. Core

The associate editor coordinating the review of this manuscript and approving it for publication was Ahmed A. Zaki Diab .

data directly measured from experiments are considered to provide the most accurate information of the reservoir. But their small sizes seem to be powerless to completely characterize reservoir with strong heterogeneity. Geophysical logging regarded as the compromise solution with high accuracy and moderate cost is considered to be indispensable and of great potential in geological stratification and reservoir evaluation especially when integrated with other means [1]–[3].

Geophysical logs reflect the reservoir information near wellbore. The logging instrument usually consists of one

transmitter and two receivers. As shown in Figure 1, signal is sent from the transmitter, reflected through the formation, and received by the two receivers respectively. The measurement will be carried out along the wellbore from the bottom to top after drilling. Signal data will be acquired point by point at an interval of 8 points/meter [4]. Repeating the measuring process by different instruments would obtain different logs. In addition to the four signals shown in Figure 1, there are 6 signals in total named gamma-ray (GR), acoustic wave (AC), density (DEN), compensated neutron logging (CNL), deep lateral logging (LLD), swallow lateral logging (LLS) respectively, and they are usually called conventional logging sequences (CLS) in general term. The CLS is considered to contain all the information in reservoir including lithology, physical property and fluids. Our goal is to determine reservoir grade and to make recommendations for perforation and fracturing. If the reservoir is poor, there is no need to spend too much for it; if the reservoir is very good, the investment should be increased to obtain the maximum benefit. Conventionally, reservoirs are classified through two steps: parameters fitting and expert evaluation. By fitting the logging data to core data (rock components, porosity, permeability, fluid saturation, etc.), experts can obtain empirical formulas and then draw cross-plots for reservoir classification. For instance, the resistivity vs. porosity cross-plot is often used to evaluate clean sand reservoirs with little shale and good physical properties. This approach suffers too much labor cost and confusion when dealing with unconventional complex reservoirs.

Machine learning (ML) with a level of automation has been adopted in logging interpretation for a long time [5]. ML algorithms can be viewed as two types: feature extraction and classification. Feature extraction includes clustering, principal component analysis (PCA), correlation analysis (CA), grey relational analysis (GRA), etc. Classification methods include artificial neural network (ANN), support vector machine (SVM), decision tree (DT), and random forest (RF) etc. These two types of methods are sometimes used in combination, and sometimes classification methods are used directly without feature extraction. For examples, Cui *et al.* [6] applied the principal component analysis (PCA) method on multiple logging signals to classify four diagenetic facies pre-defined by samples from a tight sandstone reservoir in the Ordos Basin, Central China. Schlanser *et al.* [7] tested a statistical clustering algorithm with geophysical logs for lithofacies classification in the Marcellus Shale. Guo *et al.* [8] proposed a combination model—three ANNs to predict porosity, permeability and shale content respectively following a neuro-fuzzy inference machine—for pay zones recognition. Many other similar studies can be seen in [9]–[12]. The main disadvantages of ML are as follow [13]:

(1) There are many methods can be used for feature extraction and classification. Different methods could produce different results on the same dataset. There is no standard and unified approach currently, so it still requires manual intervention to select ML method.

(2) Due to its own reasons, machine learning has limited ability to extract features and the classification accuracy is also limited. Even it may not work applied to complex reservoirs.

Requiring little manual effort and with good performance, deep learning (DL) has been attracting more attention in recent years. In earth science field, remote sensing images processing [14]–[16] and seismic images feature extraction [17]–[19] have widely adopted DL approach especially the convolutional neural network (CNN). For geophysical logging interpretation, in 2017, Li and Misra [20] built a variational auto-encoder (VAE) to predict NMR-log T2 distribution directly from several log signals. In 2018, they proposed another way of integrating several DL methods combination to generate NMR-log T2 distribution [21]. An and Cao [22] established a simple network using multiple logging signals to identify lithology. In 2020, Lin *et al.* [23] has studied automatic lithology identification by applying long short-term memory (LSTM) network to logging data. In light of 1D geophysical-logging signal can be converted from time domain to the frequency or time-frequency domain, then the converted 2D data viewed as images can be processed by CNN easily. So in 2018, Zhu *et al.* [24] combined wavelet decomposition (WD) and CNN to convert the problem of logging lithological interpretation to a supervised image recognition task. In 2020, Chen *et al.* [25] proposed a methodology combining short-time Fourier transform (STFT) and CNN for complex formation lithology identification by using drilling string vibration data. Until now, there are few literatures on DL applying to logging data. We realize some drawbacks applying DL to logging data as follow.

(1) Unlike seismic and remote sensing images, logging data are in one dimension. There are two possible solutions: ① Convert 1D to 2D form and then use 2D-CNN like [24] and [25]. But the conversion method equivalent to feature extraction will increase labor cost and may lose information. It's kind of like a ML process. ② Directly apply DL to deal with 1D data. Reference [23] used LSTM dealing with GR signal to recognize the rock facies. The LSTM is good at processing sequential signals, such as text, speech or rock sedimentary facies especially inferring the next data from the current one along the data sequence. While reservoir classification seems to be more concerned with how to integrate the six signals and extract hydrocarbon information from them.

(2) The main difference between 2D-CNN and 1D-CNN is that 1D-CNN slides the convolution window in only one dimension. Comparing to LSTM, 1D-CNN is supposed to be a better fit for reservoir classification: It doesn't pay too much attention to the signal sequence itself, but focuses on feature extraction from the whole signals combination. Nevertheless, 1D-CNN also has inadaptability: ① For the input, artificial operation is still required to divide the whole logging sequence into segments and each segment will be treated as one sample. Samples would have various sizes for their different layer thickness. While 1D-CNN requires all samples must be converted to a uniform size before input, which will

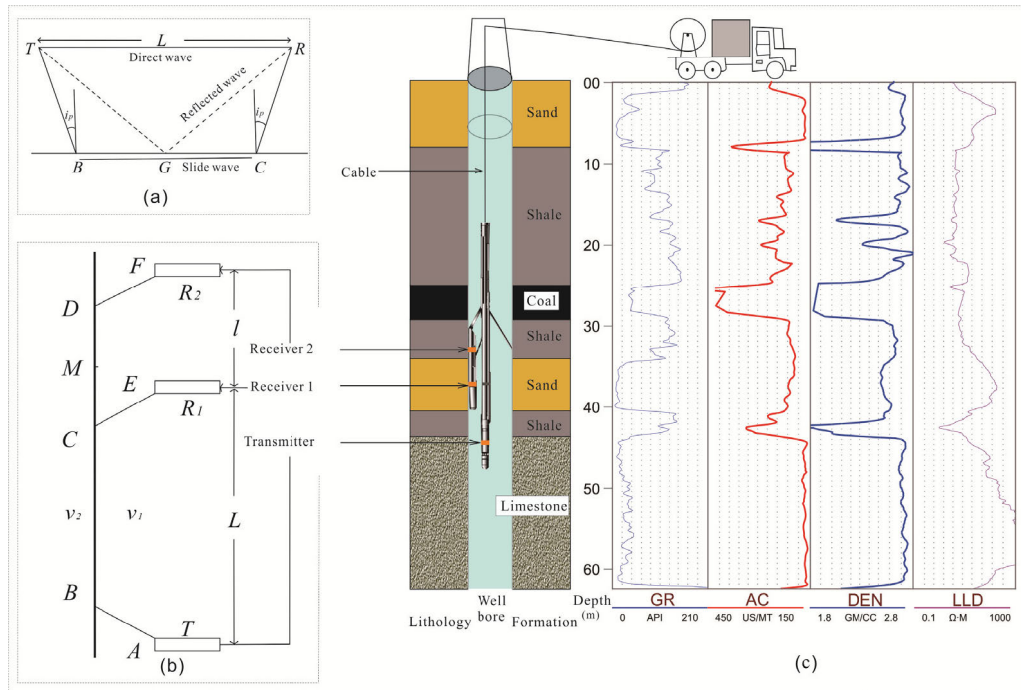


FIGURE 1. Geophysical logging diagram for reservoir classification. (a) Signal propagation. (b) Instrument components. (c) Measuring & logging curves.

bring errors or information loss. ② For the output, one sample can contain multiple data points, but only has one label as output. That’s inconsistent with the logging principle to some extent and will affect the accuracy. According to logging principles as shown in Figure 2, each logging point having its own label seems more reasonable and helps improve accuracy.

Fully convolutional network (FCN) was first proposed and applied to 2D image segmentation in 2015 [26]. It provides an approach for single point pixel classification. Based on FCN, U-net [27] for medical image segmentation was proposed. Then SegNet [28], Deeplab [29] and other algorithms were proposed after improvements. FCN has been successfully applied to SAR [30], aerial images [31], hyper-spectral images [32], seismic images [33] etc. Considering (1) and (2) comprehensively, the authors propose a 1D fully convolutional network (1D-FCN) to characterize reservoir properties. The model can receive any size input of layer thickness without manually aligning it to the same size. The result for tight gas application from 1D-FCN is better than that from other methods. For the first time in this paper, we make a detailed and in-depth comparison study on five networks by using general metrics. The contributions of this paper are summarized as follow.

(1) Structures of the five networks including two fully connected networks (global mapping neural network, GM-ANN and point-to-point mapping neural network, PPM-ANN), two fully convolutional networks (1D fully convolutional network with decision-level fusion, 1D-FCN-DEF and 1D fully convolutional network with data-level fusion, 1D-FCN-DAF)

and 1D convolutional neural network (1D-CNN). They are evaluated the suitability for processing logging data in detail.

(2) The SMOTE (synthetic minority class sampling technology) method is used to augment data and address data imbalance for the tight gas reservoir in Ordos Basin, China.

(3) The 5-fold cross validation and leave-only-one cross validation (LOOCV) are implemented for the five networks on the expanded dataset. The results are illustrated by receiver operating characteristics (ROC) curves, and the areas under the curve (AUC) are calculated to evaluate the networks quantitatively.

To sum up, three ways to reservoir classification based on logging data are shown in Figure 2. The remainder of this paper is organized as follows. The fundamentals of CNN or FCN are provided in Section II. Structures of GM-ANN, PPM-ANN, 1D-CNN, 1D-FCN-DEF and 1D-FCN-DAF are illustrated and data are augmented by SMOTE in Section III. Application results and case study in Ordos Basin of China are discussed in Section IV. We draw the conclusions and the future work in Section V.

II. FUNDAMENTALS

Should the convolution in CNN be better suited to describe reservoir characteristics than the fully connected operation in ANN? Generally thinking, reservoir properties of a certain depth d can be described by logging data at just the depth point d . Actually, as shown in Figure 1(b), reservoir parameters at the point M in the middle of CD are calculated from logging data between the two receivers as averages. In other word, the “sweet-spots” depending on the sands’ properties

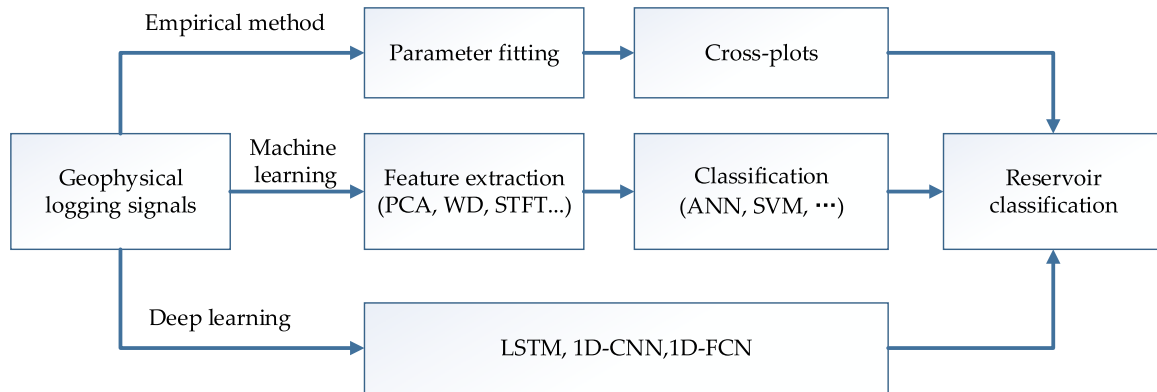


FIGURE 2. Three ways from geophysical logging signals to reservoir classification.

are implied not in the logging “point” but “segment”. It will be more reasonable the reservoir properties at depth d are implicated in an adjacent region of d expressed as $[d - a, d + a]$. However this fact is largely ignored by the fully connected ANNs.

Convolutional operation is considered be better to extract the local features. The fully convolutional neural network is a three-stage neural network without fully connected layer. The stage of feature compression contains multiple convolutional, activation and pooling layers. The stage of feature recovery can reconstruct each feature map from stage-one to original dimension through de-convolution operations. Each point will be corresponded to probabilities vector predicted from the softmax operation in the last classification stage. The theory of 1D-FCN is briefly introduced in this section, and the functions of each type of layer are described below. More details on FCN can be found in [26].

A. CONVOLUTIONAL OPERATION

One-dimensional convolutional operation is used in this paper. The convolution kernel will scan only along depth axis of the logging signal. There can be several kernels in one convolutional layer. These kernels will result in multiple channels or features called the feature map. The convolution process is described as follows:

$$h_{l,i} = X_{l-1} * W_{l,i} + b_l \tag{1}$$

where the notation $*$ denotes the dot product of the kernel and the local regions, W_i^k represents the weights matrix of the i -th kernel in l -th convolutional layer. b_l denotes the bias vector of l -th convolutional layer.

B. ACTIVATION OPERATION

After the convolution operation, activation function enables the network to acquire a nonlinear expression of the input signal to enhance the representation ability and make the learned features more dividable. Rectified Linear Unit (ReLU) is widely used as activation unit to accelerate the convergence of the CNNs. It makes the weights in the shallow layer more

trainable when using back-propagation learning method to adjust the parameters. The formula of ReLU is described as follows.

$$f(h_{l,i}) = \max\{0, h_{l,i}\} \tag{2}$$

where $h_{l,i}$ is the output value of convolutional operation after batch normalization(BN) and f is the activation of $h_{l,i}$.

C. POOLING OPERATION

In order to reduce parameters number and prevent overfitting, pooling operation is required following the convolution and activation. Max pooling is one of the most commonly used pooling methods.

$$X_l = \max(h_l^j, h_{l,i}^{j+1}) \tag{3}$$

where h_l^j represent the j -th bunch of channels vector in l -th layer. And X_l is the final output of l -th layer which has the dimension as a half of X_{l-1} .

D. DECONVOLUTIONAL OPERATION

VGG-net [34] is used in this paper. In this model, the size of feature map will be reduced by half after each convolution & pooling layer. Up-sampling called de-convolutional operation will be adopted in order to restore the same size of output as the input. The principle of de-convolutional operation as the one-dimensional linear interpolation method is shown in Figure 4.

E. SOFTMAX OPERATION

Each depth point of the full CNN would output a probability vector with the dimension the same as the number of reservoir categories. Each probability vector will be obtained by Softmax formula below.

$$\begin{aligned}
 P(Y = k | X_L, W, b) &= \text{softmax}_k(W * X_L + b) \\
 &= \frac{e^{W_k * X_L + b_k}}{\sum_{n=1}^N e^{W_n * X_L + b_n}} \tag{4}
 \end{aligned}$$

where X_L represents the input from some layer; k represents reservoir category (GAS or NO-GAS for tight gas reservoir);

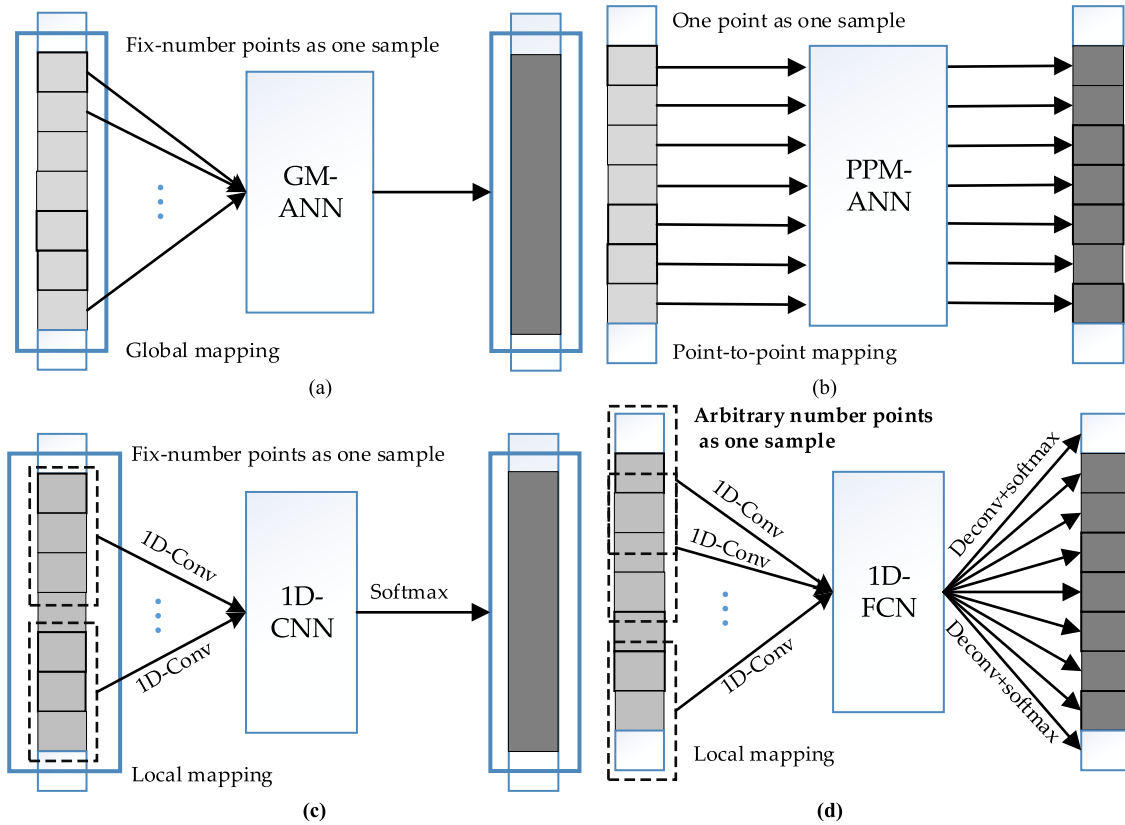


FIGURE 3. Schematic diagram of different network structures. (a) Global mapping ANN (GM-ANN). (b) Point-to-point mapping ANN (PPM-ANN). (c) 1D-CNN. (d) 1D-FCN.

W is the weight matrix, and b is the bias; $P(Y = k | X_L, W, b)$ is the conditional probability that the output Y is class k when the input is X_L .

F. NEURONS DROPOUT

Dropout is a trick proposed by Srivastava *et al.* [35] to prevent the network from overfitting. It is extremely simple but effective. The main idea is to randomly deactivate neurons along with their connections with neurons in the next layer with some probability p (a hyperparameter), which proves to be able to prevent units from co-adapting too much. In this paper, p will be set 0.5 (each neuron has a 50% chance of not working). It should be noted that dropout is only used in the training stage. All neurons work normally in the prediction stage.

III. PROPOSED MODELS

This section will describe the five network structures including two fully-connected networks (GM-ANN & PPM-ANN), two fully-convolutional networks (1D-FCN-DAF & 1D-FCN-DEF) and the common 1D-CNN.

A. BASIC NETWORK STRUCTURES

Different network structures are used for specific scenarios. As shown in Figure 3, hydrocarbon properties of the whole reservoir are considered to be hidden in all logging data

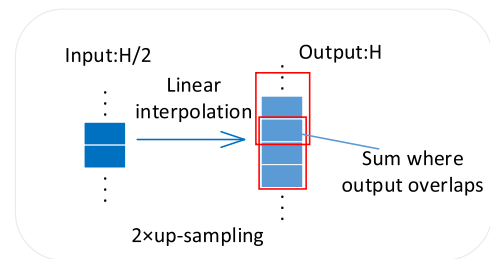


FIGURE 4. Schematic of 1D de-convolution.

throughout the entire interval. So multiple points as a whole would be taken as one sample by using a globally mapped network as shown in Figure 3(a). Point-to-point networks are often used to predict rock type, porosity, permeability or TOC etc. (Figure 3(b)).

In light of the reservoir information at one certain depth point is the average between the two receivers interval near just this depth point (seen in Figure 1(b)), CNN is well suited to this situation. The 1D-CNN shown in Figure 3(c) provides the approach to extract local features. This kind of model has been applied in biometric recognition based on multiple sensors data [36], fault diagnosis of rotating machinery from multi-signals [37], multivariate abnormal detection for industrial control systems [38], non-contact medical

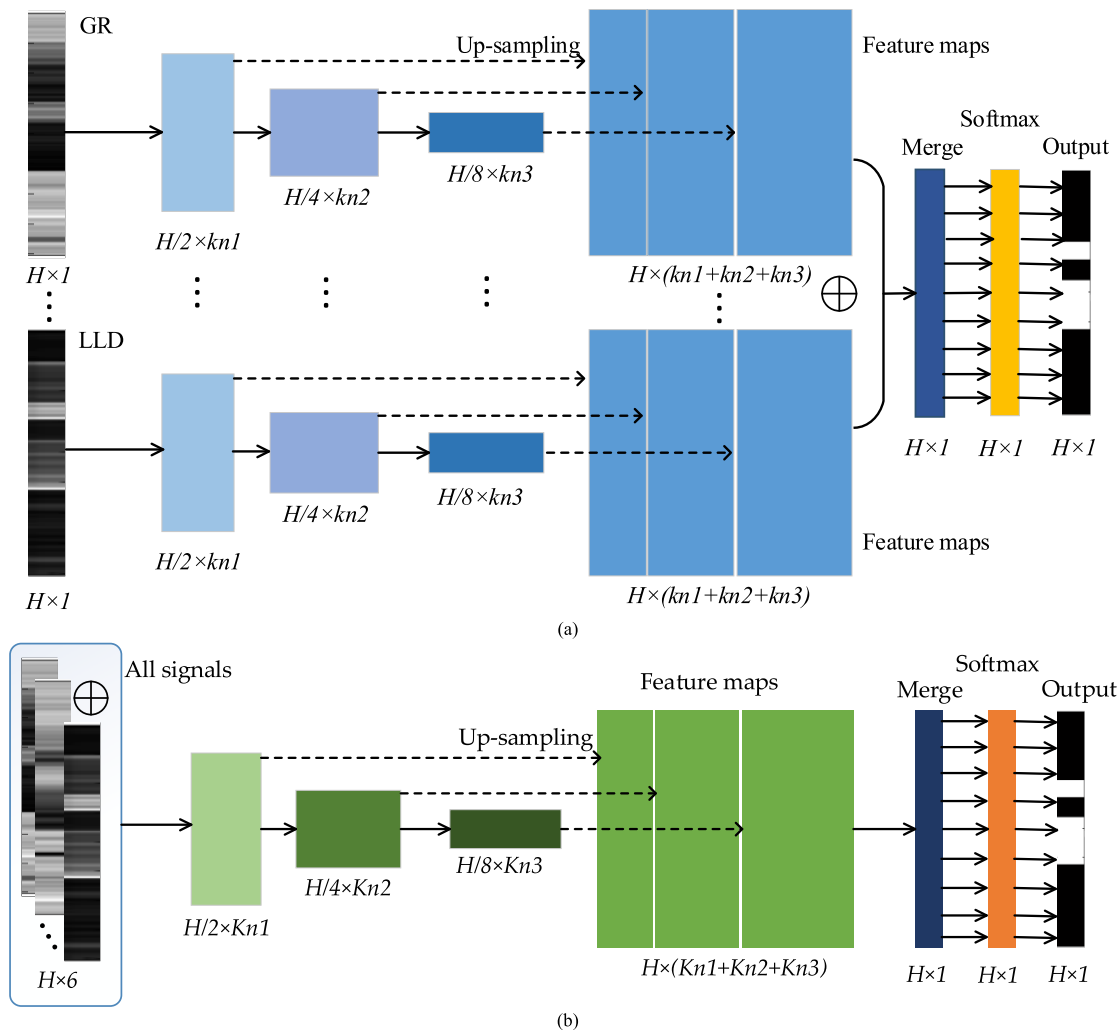


FIGURE 5. Two fusion approaches of 1D-FCN. (a) 1D-FCN with decision-level fusion (1D-FCN-DAF). (b) 1D-FCN with data-level fusion (1D-FCN-DAF).

detection based on sensors data [39], and radar jamming signal classification from one signal [40].

By integrating the advantages of CNN and point-to-point ANN, 1D-FCN can not only extract local features, but also predict the classification vector of each depth point. As shown in Figure 3 (d), the de-convolution operation is used to restore feature maps to the same size as the input. Then the softmax layer gives the prediction for every point. So fully CNN would accept any different sizes of input. These advantages fits well with the principle of logging measurement and will be introduced in detail below.

B. ARCHITECTURES OF 1D-FCN

VGG-net has been adopted as the basic network architecture. The input is sub-sampled to feature map through convolution & pooling operations layer by layer, and all layers will be up-sampled to the same dimension as the original input uniformly by de-convolutions. Furthermore, as shown in Figure 4, two fusion approaches have been proposed and

discussed in this paper. Figure 5(a) has shown the decision-level fusion. Each logging signal will be treated respectively through conv-pooling operations to generate feature maps which will be restored to original dimension as the input by de-convolution operations. Then all the feature maps will be merged into the size $H \times 1$ by convolution with the kernel size of $(kn1 + kn2 + kn3) \times 1$ in which $kn1$, $kn2$, $kn3$ are the kernel numbers. For another approach of data-level fusion in Figure 5(b), all the six signals treated together as a 2D-map at the beginning. The main differences between the two fusion approaches are that kernel sizes are $KS \times 1$ and $KS \times 6$, and the feature maps sizes are $H \times (kn1 + kn2 + kn3) \times 6$ and $H \times (Kn1 + Kn2 + Kn3)$ respectively.

During training, cross entropy loss is calculated to evaluate the differences between predicted outputs from the built model and true labels, denoted as

$$L(W, b) = \sum_{t=0}^{|D|} \log(P(Y = y^{(t)} | X^{(t)}, W, b)) \quad (5)$$

TABLE 1. Structures comparison of network.

Network	Input size	Basic structure parameters	Output Size
GM-ANN	$H \times 6$	FC1: $(H \times 6) \times 20$; FC2: 20×10	1
PPM-ANN	$1 \times 6(h)$	FC1: $(1 \times 6) \times 20$; FC2: 20×10	$1(h)$
1D-CNN	$H \times 6$	K1: 3×6 (10); K2: 3×10 (20); K3: 3×20 (40);	1
1D-FCN-DEF	$h \times 1$ (totally 6)	K1: 3×1 (10); K2: 3×10 (20); K3: 3×20 (40); Feature-maps: $H \times 70(10+20+40)$	$h \times 1$
1D-FCN-DAF	$h \times 6$	K1: 3×6 (10); K2: 3×10 (20); K3: 3×20 (40); Feature-maps: $H \times 70(10+20+40) \times 6$	$h \times 1$

where D represents log data set, and $L(W, b)$ is the sum of cross entropy loss functions. Based on training data, model parameters are updated to minimize the loss function. The optimization algorithm called adaptive moment estimation (Adam) [41] is adopted in this paper. It is an alternative method for classical stochastic gradient descent considering both the first and second moments of the gradients which achieves fast convergence that gains efficiency in computation.

C. DATA AUGUMENTATION

Data is the basis of implementing the model. The data used in this paper are from typical unconventional gas reservoir in Ordos Basin, which are characterized by complex rock types, tight rock and very low porosity. The 399 samples were obtained including logging data and corresponding gas-testing data. According to the testing results, the labels of samples include: oil layer, gas layer, oil-bearing layer, gas-bearing layer, water-bearing layer, dry layer, etc. They are re-classified into two categories of GAS and NO-GAS so as to alleviate the sample shortage of each class. Another advantage of doing this is to make it easier to compare the algorithm performances for binary classification problem.

A number of samples are required to obtain better fitting ability. U-net [27] only had 30 2D images as samples and overlap-tile method was used for data enhancement. Actual field samples with small population often have strong imbalance also. There would be less GAS samples in the early stage of exploration and less NO-GAS samples at the later stage. Generally there are three ways to overcome imbalance: sub-sampling, re-sampling, and data synthesis. Sub-sampling method randomly selects samples from the larger class to meet the sample population as the smaller class. Re-sampling method repeats sample selection from the smaller class. These two ways are more suitable for a large sample population. By mining the relationships between samples to generate new data, synthesis method is considered to be the most suitable way when the amount of logging data is small and

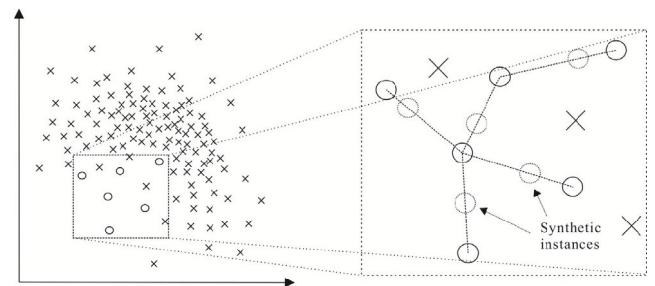


FIGURE 6. A two-dimensional example of SMOTE.

the distribution is sparse. SMOTE is one of the most popular data synthesis method.

The idea of SMOTE is as follows: (1) K -nearest neighbor (KNN) algorithm is used to calculate the K nearest neighbors of each sample; (2) N samples are randomly selected from K nearest neighbors for random linear interpolation to generate new samples; (3) Newly synthesized samples are added to the original set of the data. (4) Loop through the steps above until the required amount is met. Since the synthetic sample is not a direct copy of the instance, so the overfitting problem can be alleviated by adding samples with a similar data distribution to the original. The number of geophysical logging samples was increased from 399 (300 labeled GAS & 99 labeled NO-GAS) to 1200 (600 for each class). Figure 6 has shown a two-dimensional example of SMOTE. The diagram on the right is showing a schematic of synthesizing data from real data where the dashed line circles represent the synthetic data obtained by random linear interpolation between the real data labeled by solid line circles. More details can be found in literature [42].

IV. RESULTS & DISCUSSION

Results on the tight gas reservoir in Ordos Basin from the five networks have been discussed in this section. The basic structural parameters are shown in Table 1. Actually, due to different reservoir thicknesses, the length of logging data is

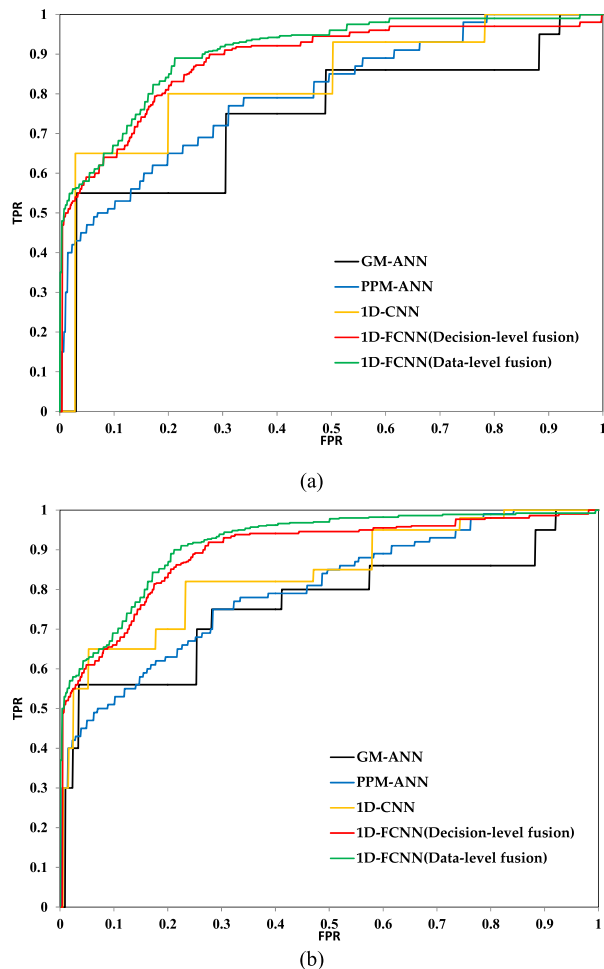


FIGURE 7. ROCs of the five networks. (a) 5-fold cross-validation. (b) LOOCV.

a variable named h . So for the input size, PPM-ANN always takes only one depth point (with 6 values) as a sample. GM-ANN and 1D-CNN need to align variable h to a same fixed value H by up- or sub-sampling operation. While 1D-FCN models can directly deal with the variable h , which are the same as the output sizes on the first dimension as shown in the last column. The output sizes from GM-ANN, PPM-ANN and 1D-CNN are all single values: reservoir categories. Table 1 also shows the basic structure parameters in the middle part. FC1: $(1 \times 6) \times 20$ means that the dimension of the first full connection layer is 6 and the output dimension is 20. K1: 3×6 (10) represents the first convolutional layer, with kernel size of 3×6 and a total of 10 convolution kernels. To ensure fairness, in the two ANNs, the hidden layers hold the same dimensions, and convolution kernels with the same sizes and numbers have been in the three CNNs. It should be noted parameters in pooling, de-convolution and Softmax layers not listed can all be inferred according to the basic parameters in Table 1.

A. CROSS VALIDATION

Let P be the probability of Softmax layer output. As a classification problem, the final output should be a label of 1

TABLE 2. Confusion matrix for binary classification problem.

Prediction	Real label	
	Positive(1)	Negative(0)
Positive(1)	True Positive	False Positive
Negative(0)	False Negative	True Negative
Percentage(%)	$TPR=TP/(TP+FN)$	$FPR=FP/(FP+TN)$

TABLE 3. AUCS from the five networks.

	GM-ANN	PPM-ANN	1D-CNN	1D-FCN-DEF	1D-FCN-DAF
5-fold	0.7433	0.8010	0.8319	0.8836	0.9054
LOOCV	0.7597	0.8002	0.8408	0.8941	0.9160
Average	0.7515	0.8006	0.8364	0.8889	0.9107

(GAS) or 0 (NO-GAS), so a rule will be established to convert probabilities to categories as shown in formula (6). y_{pred} represents the class of the highest probability in prediction results. $V_{threshold}$ is a value between 0 and 1.

$$y_{pred} = \begin{cases} 1(GAS) & P \geq V_{threshold} \\ 0(NO-GAS) & P < V_{threshold} \end{cases} \quad (6)$$

True positive rate (TPR) and false positive rate (FPR) are two common indicators for binary labeling problem. TPR denotes the percentage of samples predicted the label of 1 in all samples with a real label of 1. While FPR represents the same percentage but in all samples with a real label of 0 (see Table 2 for details). By plotting the TPR against the FPR at different thresholds according to formula (2), we will get a curve called Receiver operating characteristics (ROC) as an aggregative indicator. We could also calculate the area under ROC curve (AUC). The value range of AUC is between 0.5 and 1. $AUC = 1$ means this method gives a perfect prediction performance while $AUC = 0.5$ indicates the performance of this method is same as random selection.

We exploited 5-fold CV and LOOCV to assess the generalization ability and robustness. In LOOCV (leave-one-out cross-validation) evaluation, each reservoir is regard as a test sample in turn while the rest reservoirs were treated as training samples. While 5-fold cross-validation divides the data set into 5 equal parts, and takes 1 part as test set in turn and other 4 parts as training set. We repeated each procedure 100 times and averaging them to produce more stable results.

The ROCs of the five networks (GM-ANN, PPM-ANN, 1D-CNN, 1D-FCN-DEF and 1D-FCN-DAF) in 5-fold cross-validation and LOOCV have been shown in Figure 7. Figure 7(a) & (b) have all shown the ROCs of GM-ANN and PPM-ANN are lower than those of the other three CNN models, which indicate it's important of applying convolutions. For 1D-FCN-DAF and 1D-FCN-DEF, the former seems to have a smoother and higher ROC curve than the

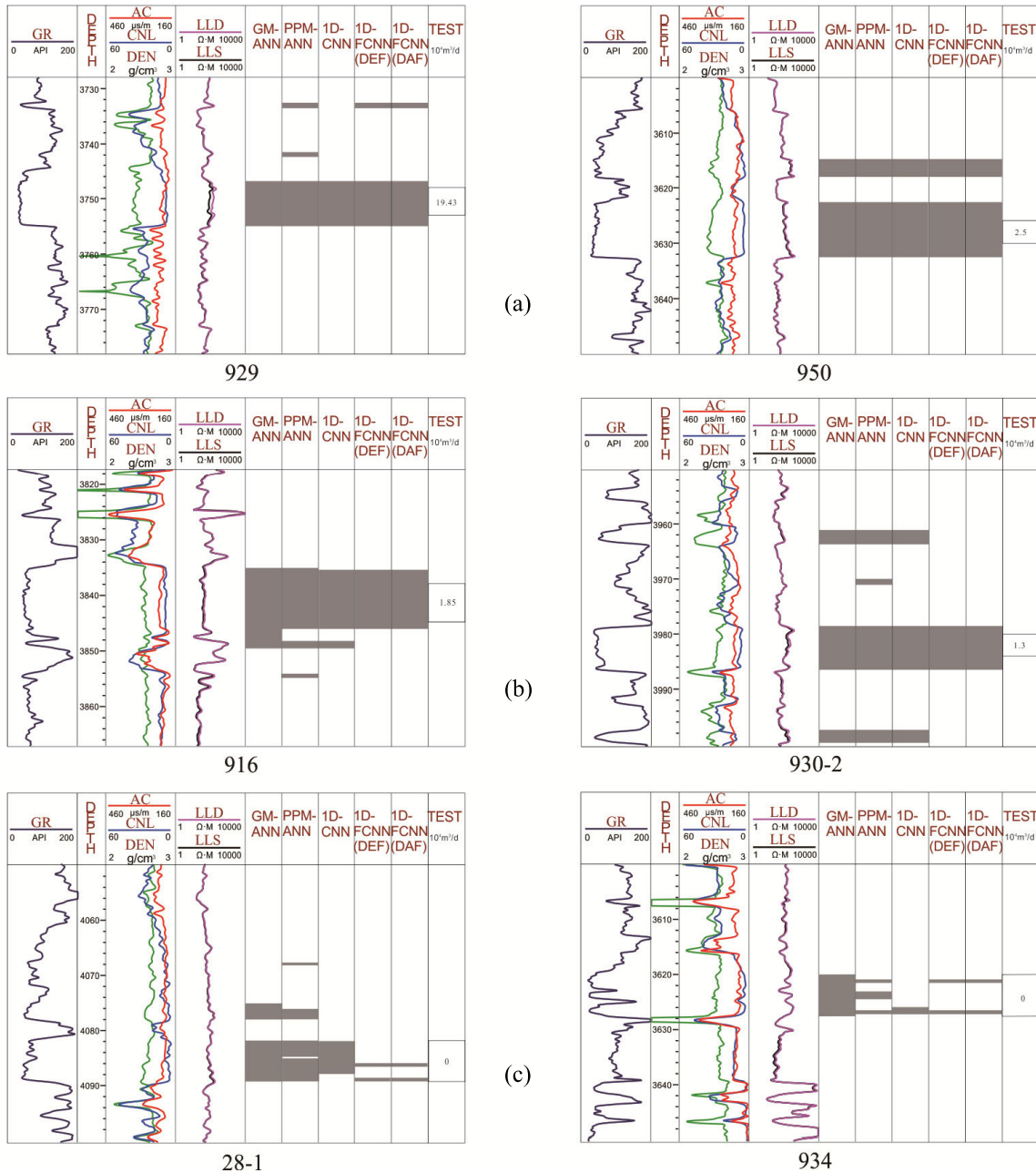


FIGURE 8. Typical cases of three reservoir types by using different methods. (a) Type-I. (b) Type-II. (c) Type III.

latter. It illustrates that features fusion at an earlier stage would result in higher accuracy and stronger robustness.

The AUCs of the five networks have been listed in Table 3. Apparently, 5-fold CV has achieved higher values than the LOOCV for all the five networks. In addition, all the three kinds of convolutional networks have achieved better results than the other two kinds of ANNs, and 1D-FCN-DAF has the best effect. This is consistent with the results from Figure 7.

B. CASE STUDY

Samples can be divided into three types according to the difference of physical properties. Type-I can be easy to iden-

tify for their good permeability. Type II has the medium permeability and porosity. So reservoir classification is also moderately difficult. Type-III has extremely poor physical properties, complex lithology leading to complex fluid properties, which are difficult to identify by common means. In this paper, several typical cases are selected respectively from each type for discussion.

As we can see in Figure 8, both layers of well #929 and well #950 have good integrity, clean sand, high porosity, and high resistivity. They are typical samples of Type-I. All the 5 nets have gotten correct predictions as TEST results. Layers in well #916 and well #930-2 have medium porosity and very low resistivity. They are partly interpreted as GAS layers

by the GM-ANN and PPM-ANN. The three CNNs have predicted them to be GAS which is consistent well with TEST results. Layers in well #28-1 and well #934 mainly compose of thin interbedded sand-mud. Reservoir complexity leads to the geophysical-logging information overlapping in a certain neighborhood and would affect GAS judgment. GM-ANN, PPM-ANN and 1D-CNN all judge it as a gas-bearing layer. While 1D-FCNs identifies them to be very thin layers with little gas and do not recommend well testing. And the final TEST conclusion is a dry layer. For better display in Figure 8, the gray color represents GAS.

V. CONCLUSION

Reservoir properties of depth point d are not only related to the current depth point logging data. According to the logging principle, the logging data at point d is actually the average value within the neighborhood interval of d . In light of this, we have introduced convolutions to neural network. Five networks, GM-ANN, PPM-ANN, 1D-CNN, 1D-FCN-DEF and 1D-FCN-DAF, have been studied. SMOTE has been applied to expand data amount from 399 to 1,200. Results of five networks with the results of 5-fold and LOOCV have been compared in detail. Results on tight gas in Ordos basin of China illustrated by receiver operating characteristics (ROC) curves show that 1D-FCN-DEF and 1D-FCN-DAF have achieved the higher area under the curve (AUC) with the values of 0.8889 and 0.9107 respectively in average comparing to 0.7515, 0.8006 and 0.8364 of the two ANNs and 1D-CNN. Case study proves that 1D-FCNs is more accurate than ANNs and 1D-CNN for complex reservoirs. This paper provides a new idea for logging interpretation and expands the application scope of DL in Geophysical-logging signals processing.

There are still some points for improvement as follow.

(1) Adjacent samples from other different classes have not taken into account by SMOTE. This would cause samples overlapping in the same class and local noises aggravation.

(2) There is not enough logging data, but there is plenty of seismic data at the early exploration stage even if they are unlabeled. How can we integrate unlabeled seismic data into labeled geophysical-logging data to further improve the accuracy is a new research topic.

(3) In fact, VGG-net is just the one classic framework for FCNs. New networks similar to the VGG-net but with better performance have been reported in some literatures. More experiments by using new networks for the problem in this paper would be carried out in future work.

REFERENCES

- [1] S. L. Luo, G. M. Hu, L. X. Li, J. W. Wang, and X. T. Li, "Genetic analysis and well-log evaluation of the productivity simulation for unconventional gas reservoirs of tight sandstone: A case from B gas reservoirs in A sag," (in Chinese), *Prog. Geophys.*, vol. 30, no. 6, pp. 2714–2722, 2015.
- [2] S. S. Yerramilli, R. C. Yerramilli, N. Vedanti, M. K. Sen, and R. P. Srivastava, "Integrated reservoir characterization of an unconventional reservoir using 3D seismic and well log data: A case study of Balol field, India," in *Proc. SEG Tech. Program Expanded Abstr.*, Sep. 2013, pp. 2279–2284.
- [3] D. Maity and F. Aminzadeh, "Reservoir characterization of an unconventional reservoir by integrating microseismic, seismic, and well log data," in *Proc. SPE Western Regional Meeting*, 2012, doi: [10.2118/154339-MS](https://doi.org/10.2118/154339-MS).
- [4] Y. Liu, C. Shi, Q. Wu, R. Zhang, and Z. Zhou, "Visual analytics of stratigraphic correlation for multi-attribute well-logging data exploration," *IEEE Access*, vol. 7, pp. 98122–98135, 2019, doi: [10.1109/ACCESS.2019.2929061](https://doi.org/10.1109/ACCESS.2019.2929061).
- [5] P.-Y. Wu, V. Jain, M. S. Kulkarni, and A. Abubakar, "Machine learning-based method for automated well-log processing and interpretation," in *Proc. SEG Tech. Program Expanded Abstr.*, Aug. 2018, pp. 2041–2045.
- [6] Y. Cui, G. Wang, S. J. Jones, Z. Zhou, Y. Ran, J. Lai, R. Li, and L. Deng, "Prediction of diagenetic facies using well logs—A case study from the upper Triassic Yanchang formation, Ordos Basin, China," *Mar. Petroleum Geol.*, vol. 81, pp. 50–65, Mar. 2017.
- [7] K. Schlanser, D. Grana, and E. Campbell-Stone, "Lithofacies classification in the Marcellus shale by applying a statistical clustering algorithm to petrophysical and elastic well logs," *Interpretation*, vol. 4, no. 2, pp. SE31–SE49, May 2016.
- [8] D. Guo, K. Zhu, L. Wang, J. Li, and J. Xu, "A new methodology for identification of potential pay zones from well logs: Intelligent system establishment and application in the Eastern Junggar Basin, China," *Petroleum Sci.*, vol. 11, no. 2, pp. 258–264, Jun. 2014.
- [9] X. Wang, S. Yang, Y. Zhao, and Y. Wang, "Lithology identification using an optimized KNN clustering method based on entropy-weighted cosine distance in Mesozoic strata of Gaoqing field, Jiyang depression," *J. Petroleum Sci. Eng.*, vol. 166, pp. 157–174, Jul. 2018.
- [10] Y. Gu, Z. Bao, X. Song, S. Patil, and K. Ling, "Complex lithology prediction using probabilistic neural network improved by continuous restricted Boltzmann machine and particle swarm optimization," *J. Petroleum Sci. Eng.*, vol. 179, pp. 966–978, Aug. 2019.
- [11] Y. Zhong, L. Zhao, Z. Liu, Y. Xu, and R. Li, "Using a support vector machine method to predict the development indices of very high water cut oilfields," *Petroleum Sci.*, vol. 7, no. 3, pp. 379–384, Sep. 2010.
- [12] S. Dong, Z. Wang, and L. Zeng, "Lithology identification using kernel Fisher discriminant analysis with well logs," *J. Petroleum Sci. Eng.*, vol. 143, pp. 95–102, Jul. 2016.
- [13] T. Merembayev, R. Yunussov, and A. Yedilkhan, "Machine learning algorithms for classification geology data from well logging," in *Proc. 14th Int. Conf. Electron. Comput. (ICECCO)*, Kaskelen, Kazakhstan, Nov. 2018, pp. 206–212, doi: [10.1109/ICECCO.2018.8634775](https://doi.org/10.1109/ICECCO.2018.8634775).
- [14] B. Petrovska, E. Zdravovski, P. Lameski, R. Corizzo, I. Štajduhar, and J. Lerga, "Deep learning for feature extraction in remote sensing: A case-study of aerial scene classification," *Sensors*, vol. 20, no. 14, p. 3906, Jul. 2020.
- [15] W. Zhao, W. Ma, L. Jiao, P. Chen, S. Yang, and B. Hou, "Multi-scale image block-level F-CNN for remote sensing images object detection," *IEEE Access*, vol. 7, pp. 43607–43621, 2019, doi: [10.1109/ACCESS.2019.2908016](https://doi.org/10.1109/ACCESS.2019.2908016).
- [16] L. Liu, M. Ji, and M. Buchroithner, "Transfer learning for soil spectroscopy based on convolutional neural networks and its application in soil clay content mapping using hyperspectral imagery," *Sensors*, vol. 18, no. 9, p. 3169, Sep. 2018.
- [17] S. Yuan, J. Liu, S. Wang, T. Wang, and P. Shi, "Seismic waveform classification and first-break picking using convolution neural networks," *IEEE Geosci. Remote Sens. Lett.*, vol. 15, no. 2, pp. 272–276, Feb. 2018.
- [18] J. Wang, X. Zheng, and H. Huang, "Seismic facies analysis based on 3D-CNN and seismic stratigraphic slice," in *Proc. SEG Tech. Program Expanded Abstr.*, Aug. 2019, pp. 2609–2613.
- [19] A. Siahkoobi, M. Louboutin, R. Kumar, and F. J. Herrmann, "Deep-convolutional neural networks in prestack seismic: Two exploratory examples," in *Proc. SEG Tech. Program Expanded Abstr.*, Aug. 2018, pp. 2196–2200, doi: [10.1190/segam2018-2998599.1](https://doi.org/10.1190/segam2018-2998599.1).
- [20] H. Li and S. Misra, "Prediction of subsurface NMR T2 distributions in a shale petroleum system using variational autoencoder-based neural networks," *IEEE Geosci. Remote Sens. Lett.*, vol. 14, no. 12, pp. 2395–2397, Dec. 2017.
- [21] H. Li and S. Misra, "Long short-term memory and variational autoencoder with convolutional neural networks for generating NMR T2 distributions," *IEEE Geosci. Remote Sens. Lett.*, vol. 16, no. 2, pp. 192–195, Feb. 2019.
- [22] P. An and D. P. Cao, "Research and application of logging lithology identification based on deep learning," (in Chinese), *Prog. Geophys.*, vol. 33, no. 3, pp. 1029–1034, 2018.

- [23] J. Lin, H. Li, N. Liu, J. Gao, and Z. Li, "Automatic lithology identification by applying LSTM to logging data: A case study in X tight rock reservoirs," *IEEE Geosci. Remote Sens. Lett.*, early access, Jun. 19, 2020, doi: 10.1109/LGRS.2020.3001282.
- [24] L. Zhu, H. Li, Z. Yang, C. Li, and T. Ao, "Intelligent logging lithological interpretation with convolutional neural networks," *Petrophysics—SPWLA J. Formation Eval. Reservoir Description*, vol. 59, no. 6, pp. 799–810, 2018.
- [25] G. Chen, M. Chen, G. Hong, Y. Lu, B. Zhou, and Y. Gao, "A new method of lithology classification based on convolutional neural network algorithm by utilizing drilling string vibration data," *Energies*, vol. 13, no. 4, p. 888, Feb. 2020.
- [26] E. Shelhamer, J. Long, and T. Darrell, "Fully convolutional networks for semantic segmentation," *IEEE Trans. Pattern Anal. Mach. Intell.*, vol. 39, no. 4, pp. 640–651, Apr. 2017.
- [27] O. Ronneberger, P. Fischer, and T. Brox, "U-Net: Convolutional networks for biomedical image segmentation," 2015, *arXiv:1505.04597*. [Online]. Available: <https://arxiv.org/abs/1505.04597>
- [28] B. Vijay, A. Kendall, and R. Cipolla, "SegNet: A deep convolutional encoder-decoder architecture for image segmentation," in *Proc. Comput. Vis. Pattern Recognit. (CVPR)*, 2015. [Online]. Available: <https://arxiv.org/abs/1511.00561>
- [29] L.-C. Chen, G. Papandreou, I. Kokkinos, K. Murphy, and A. L. Yuille, "DeepLab: Semantic image segmentation with deep convolutional nets, atrous convolution, and fully connected CRFs," *IEEE Trans. Pattern Anal. Mach. Intell.*, vol. 40, no. 4, pp. 834–848, Apr. 2018.
- [30] E. Nemni, J. Bullock, S. Belabbes, and L. Bromley, "Fully convolutional neural network for rapid flood segmentation in synthetic aperture radar imagery," *Remote Sens.*, vol. 12, no. 16, p. 2532, Aug. 2020.
- [31] W. Song, B. Zhong, and X. Sun, "Building corner detection in aerial images with fully convolutional networks," *Sensors*, vol. 19, no. 8, p. 1915, Apr. 2019.
- [32] Z. Niu, W. Liu, J. Zhao, and G. Jiang, "DeepLab-based spatial feature extraction for hyperspectral image classification," *IEEE Geosci. Remote Sens. Lett.*, vol. 16, no. 2, pp. 251–255, Feb. 2019.
- [33] T. Xie, Y. Zhao, X. Jiao, W. Sang, and S. Yuan, "First-break automatic picking with fully convolutional networks and transfer learning," in *Proc. SEG Tech. Program Expanded Abstr.*, Aug. 2019, pp. 4972–4976.
- [34] K. Simonyan and A. Zisserman, "Very deep convolutional networks for large-scale image recognition," 2014, *arXiv:1409.1556*. [Online]. Available: <http://arxiv.org/abs/1409.1556>
- [35] N. Srivastava, G. Hinton, A. Krizhevsky, I. Sutskever, and R. Salakhutdinov, "Dropout: A simple way to prevent neural networks from overfitting," *J. Mach. Learn. Res.*, vol. 15, no. 1, pp. 1929–1958, 2014.
- [36] S. Bianco and P. Napolitano, "Biometric recognition using multimodal physiological signals," *IEEE Access*, vol. 7, pp. 83581–83588, 2019.
- [37] Y. Li, L. Zou, L. Jiang, and X. Zhou, "Fault diagnosis of rotating machinery based on combination of deep belief network and one-dimensional convolutional neural network," *IEEE Access*, vol. 7, pp. 165710–165723, 2019.
- [38] X. Xie, B. Wang, T. Wan, and W. Tang, "Multivariate abnormal detection for industrial control systems using 1D CNN and GRU," *IEEE Access*, vol. 8, pp. 88348–88359, 2020.
- [39] L. Guan, F. Hu, F. Al-Turjman, M. B. Khan, and X. Yang, "A non-contact paraparesis detection technique based on 1D-CNN," *IEEE Access*, vol. 7, pp. 182280–182288, 2019.
- [40] G. Shao, Y. Chen, and Y. Wei, "Convolutional neural network-based radar jamming signal classification with sufficient and limited samples," *IEEE Access*, vol. 8, pp. 80588–80598, 2020.
- [41] D. P. Kingma and J. Ba, "Adam: A method for stochastic optimization," 2014, *arXiv:1412.6980*. [Online]. Available: <http://arxiv.org/abs/1412.6980>
- [42] N. V. Chawla, K. W. Bowyer, L. O. Hall, and W. P. Kegelmeyer, "SMOTE: Synthetic minority over-sampling technique," *J. Artif. Intell. Res.*, vol. 16, pp. 321–357, Jun. 2002.



KAI ZHU received the bachelor's degree in information and computer science, and the master's and Ph.D. degrees in petroleum engineering computing technology from the China University of Petroleum, China, in 2008, 2011, and 2014, respectively. He is currently a Teacher with the Qingdao University of Technology. His research interests include machine learning algorithms and its applications, and big data analysis related to oil and gas exploration and development.



YONGHUI DU received the bachelor's degree in resource exploration and engineering (energy) and the master's degree in oil and natural gas engineering from the China University of Geosciences, Beijing, in 2011 and 2014, respectively. She is currently a Geological Engineer with Research Institute of Shaanxi Yanchang Petroleum (Group) Company Ltd. Her research interests include gas development geology, clastic sedimentology, and reservoir logging interpretation.



QIAN WANG was born in Heze, China, in 1988. He received the master's degree in prospecting and exploration for oil and gas from the China University of Petroleum, Qingdao, China, in 2014. He is currently a Researcher with Research Institute of Shaanxi Yanchang Petroleum (Group) Company Ltd., Xi'an, China. His current research interests include gas development geology, clastic sedimentology, and reservoir logging interpretation.



NAIHUA JI received the bachelor's degree in computer science and technology and the master's degree in software and theory from Yanshan University, in 1997 and 2004, respectively. He worked as an Intern with Beijing Bixi Radio and Television Technology Company Ltd., for one and a half year, and has been teaching at the Qingdao University of Technology since 2004. His research interests include reinforcement learning, integrated manufacturing, and enterprise informatization.



LI ZHANG received the bachelor's degree in computer science and the master's degree in computer software and theory from Shandong Normal University, in 2004 and 2007, respectively. She is currently a Teacher with the Qingdao University of Technology. Her research interests include machine learning and big data analysis.